Segmentation of the Left Ventricular Endocardium and Epicardium

Project Report: Medical Sensors & Digitization

6 January, 2019

Abstract

The project recreates, modifies and proposes an alternative method of fast, fully automatic segmentation of the left ventricular (LV) endocardium and epicardium from the end-diastolic/systolic (ED/ES) phase images of a short-axis cardiac cine-MRI sequence. By performing a time-based, automatic localization of the heart, followed by a combination of the Chan-Vese active contours method, k-means algorithm and classification via roundness metric, the LV mask in ED is created. The LV mask in ES is generated from the ED segmentation, using a similar approach. Furthermore, the LV myocardium in ED is segmented using the LV mask in ED, via polar transformation and convolution. For the training set of MICCAI 2017 ACDC Challenge, a mean Dice Index of 0.92 and 0.85 have been obtained for a mid-ventricular phase slice in ED and ES, respectively, for all definitive results (96 out of 100 patients). Meanwhile, the equivalent Hausdorff Distance is calculated 3.88 and 4.65 for ED and ES, respectively.

Anindya Shaha

Ahmed Gouda

MSc. Medical Imaging and Applications (MAIA)
Centre Universitaire Condorcet
Université de Bourgogne

Contents

1 Introduction

1.1 Objectives

The project is based on the **Automated Cardiac Diagnosis Challenge (ACDC)** [1] of the annual International Conference on Medical Image Computing & Computer Assisted Intervention (MICCAI). The core objective is to perform semi-automatic/automatic segmentation of the left ventricular endocardium and epicardium on each diastolic and systolic image of a short-axis cardiac cine-MRI sequence.

The research paper [2] inspiring this particular approach is titled *"Fully-Automatic Cardiac Segmentation in MRI Using MRF Model Optimization, Substructures Tracking and B-Spline Smoothing"*, from the MICCAI 2017 ACDC Challenge, as published by Elias Grinias and Georgios Tziritas from the University of Crete, Greece.

1.2 Preamble Repositories

The following online repositories have been set up to facilitate communication and the cross-coordination of resources over the course of the project:

- **Google Drive** (Cloud Storage): `http://bit.ly/2GZfinE`
- **BitBucket** (Code Repository): `http://bit.ly/2GPWXJx`

1.3 Dataset

The training dataset consists of one end diastole (ED) and one end systole (ES) frame for 100 patients, each of which contain multiple slices covering the whole heart, along the axial plane. The slices are available in Nifti format and they are accompanied by the corresponding ground truth for segmentation, as manually charted by medical experts.

2 Methodology

The complete methodology is divided into 3 parts, based on each of the cardiac structures segmented. Using a combination of the **Chan-Vese active contours method** [3], ***k-means* algorithm**, **roundness metric** and **polar transformation**, the objective is accomplished for the myocardium in the ED phase and the left ventricle in both the ED and ES phases. The target slice used for demonstration is the mid-ventricular slice (1/3 position in z axis) in ED/ES phases, owing to their clear definition of both ventricles. However, the proposed method is generally applicable for any slice.

2.1 Segmentation of Left Ventricle in ED Phase

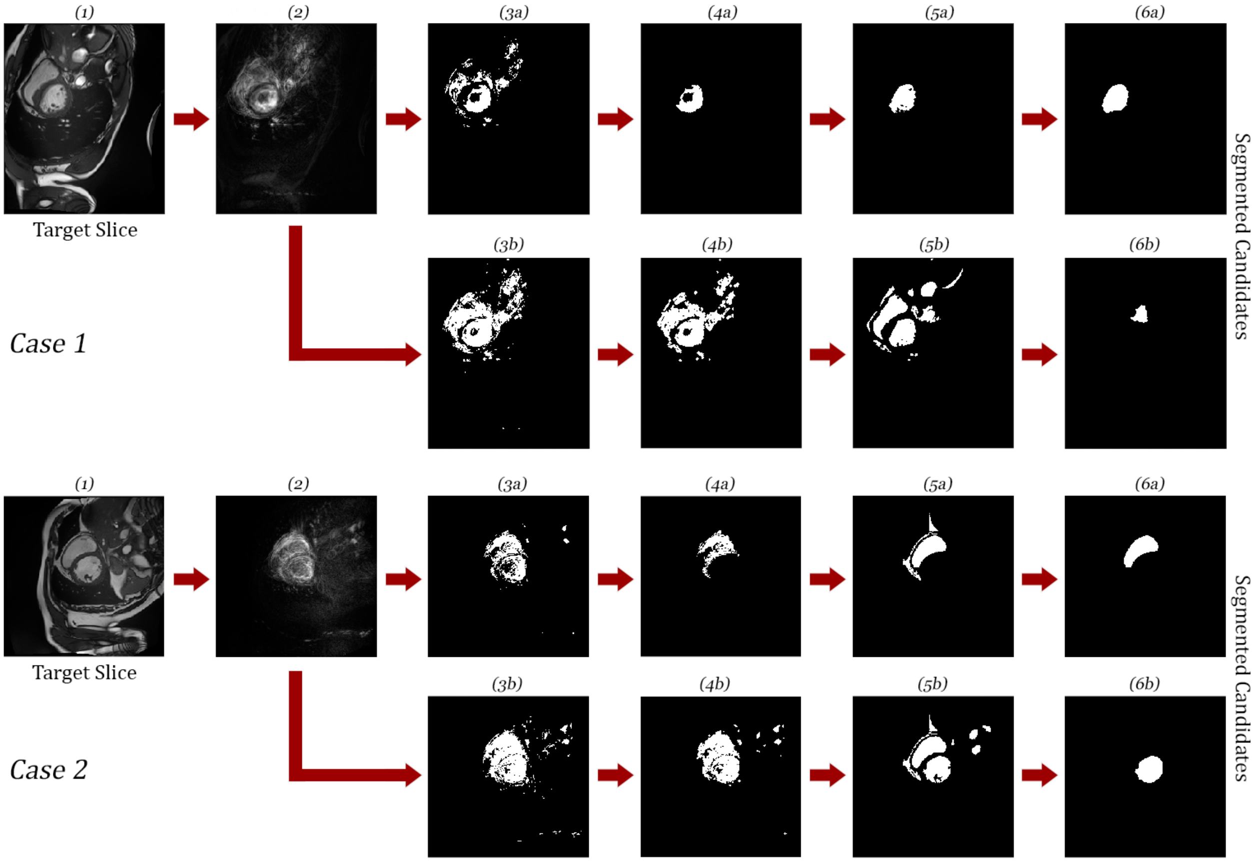

Figure 1: Sequence of operations for the parallel algorithms, `Alg1` (3a) and `Alg2` (3b), computing the segmented masks in ED mid-ventricular phase, for 2 difference cases.

Automatic Localization of the Heart

- Ideally, the heart is the only moving organ in the sequences. Hence, by using a time-based approach and taking the **mean absolute difference between corresponding slices in the ED and ES phases**, we obtain an intensity image highlighting the heart [Fig 1:*(2)*].

- From this point onward, our method diverges from the reference paper by using two parallel algorithms instead of one, each suited for a different scenario. In `Alg1`, we simply threshold the intensity image at 30% [Fig 1:*(3a)*]. For `Alg2`, we threshold it by 20% and then dilate it [Fig 1:*(3b)*]. This generates two different localized images of the heart.

Extraction via Active Contours & K-Means

- The remaining steps are the same for both `Alg1` and `Alg2`. First, the largest connected component in Fig 1:*(3)* is extracted. For an isointense localized image of the heart

[Fig 1:*Case2,(2)*], using `Alg1`, the largest connected component is more likely to be the right ventricle or its surroundings [Fig 1:*Case2,(4a)*]. But `Alg2` is more likely to extract the entire heart [Fig 1:*Case2,(4b)*]. This is because the image dilation applied in `Alg2`, connects the relatively smaller left ventricle component with the larger surrounding mass. Alternately, for a localized image with a hyperintense left ventricle [Fig 1:*Case1,(2)*], the opposite is true. `Alg1` extracts the left ventricle [Fig 1:*Case1,(4a)*], while `Alg2` extracts additional surrounding components [Fig 1:*Case1,(4b)*].

- Next, using the largest extracted component as a mask, we apply **Chan-Vese active contours** on the target slice to segment the heart. The resulting image is masked with the extracted component once more and quantized into two levels, using ***k-means* with 'cityblock' distance**. This produces our segmented images in Fig 1:*(5)*.

Classification via Roundness Metric

- To extract the left ventricle, which is typically ellipsoid in shape [4], we process (morphological 'close', fill holes, remove branches), label and classify all segmented objects in each image [Fig 1:*(5)*], based on their roundness metric [5]. We evaluate this, using their **circularity index**, **eccentricity**, **ratio of major/minor axial lengths** and areas (assigning each parameter with a different weight, based on testing and fine-tuning for optimal results). By extracting the most 'round' object, ideally, we obtain our final segmented mask for the left ventricle.

- However, we can see this is not always the case for a given algorithm. In *Case 1*, `Alg1` creates the correct mask [Fig 1:*Case 1,(6a)*], whereas in *Case 2*, `Alg2` performs better [Fig 1:*Case 2,(6b)*]. Hence, parallel computation of both algorithms is necessary for our given approach. In the final step, we classify and extract based on the roundness metric once more, but this time not between objects in the same image, but rather between the segmented candidates from each algorithm. The result is a mask of the left ventricle endocardium.

2.2 Segmentation of Left Ventricle in ES Phase

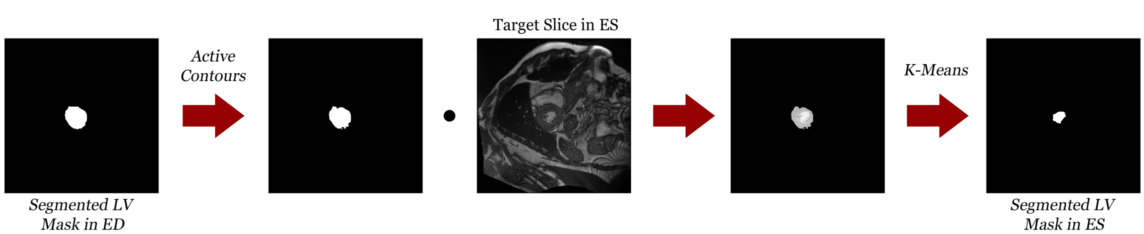

Figure 2: Sequence of operations to compute the segmented mask in ES mid-ventricular phase, using the mask generated in ED phase.

Extraction via Active Contours & K-Means

- To segment the left ventricle in the ES phase, we use the segmentated mask generated for the same slice in the ED phase. First, we perform active contours on the target slice in ES, using the segmented mask in ED. We multiply the resulting image with a normalized image of the target slice. This produces an estimate of our left ventricle, including portions of the myocardial wall.
- Next, we apply *k-means* with 'cityblock' distance and quantize the image into two levels. The output image, upon post-processing and cleanup, will be the segmented mask for the left ventricular endocardium in the ES phase. This process has been illustrated in Fig 2.

2.3 Segmentation of Myocardium in ED Phase

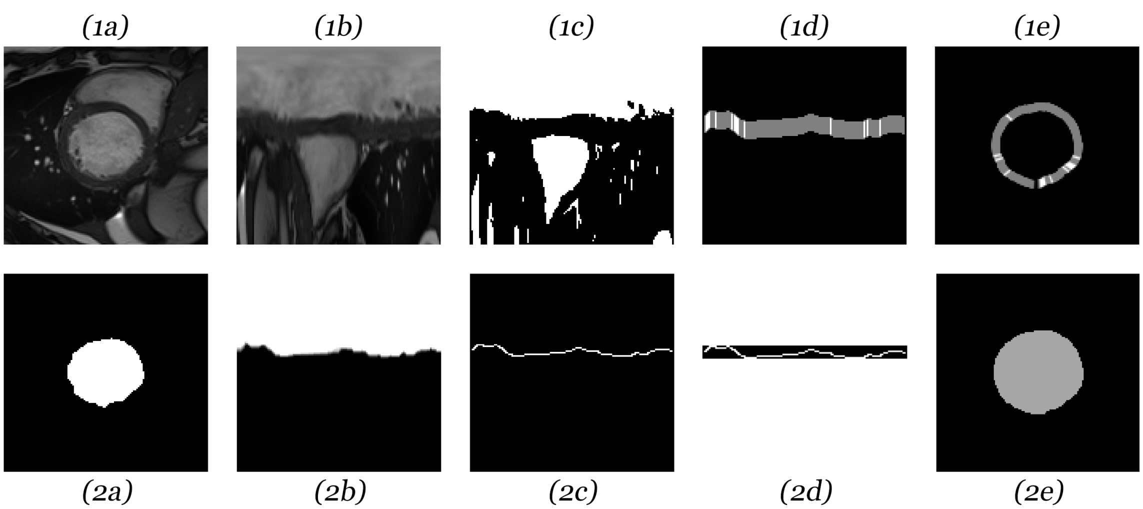

Figure 3: Sequence of operations for segmentation of the myocardium using the left ventricular mask in the ED mid-ventricular phase.

Polar Transformation

- The segmentation process for the myocardium is started with a polar transformation [Fig 3:*(1b,2b)*] of the target slice and the segmented mask obtained for the left ventricular endocardium in the previous stage.
- Next, the transformed slice is binarized [Fig 3:*(1c)*], while for the transformed mask, we apply **'canny' edge detection** [6] [Fig 3:*(2c)*].

Convolution & Thresholding

- We apply convolution on the binarized slice, using the extracted edge as a filter [Fig 3:*(2d)*]. From the resulting response, we set a threshold to extract the predicted myocardial wall. For the final program, we have defined this threshold as **0.07** to ensure a fair balance of sensitivity and specificity, and generate optimal results across the entire dataset. This process has been illustrated in Fig 4.

- By transforming the resulting image back to cartesian coordinates, we have the segmented myocardial wall [Fig 3:*(1e)*]. The image is further cleaned, filled and processed to generate the final segmented mask of the left ventricular epicardium [Fig 3:*(2e)*].

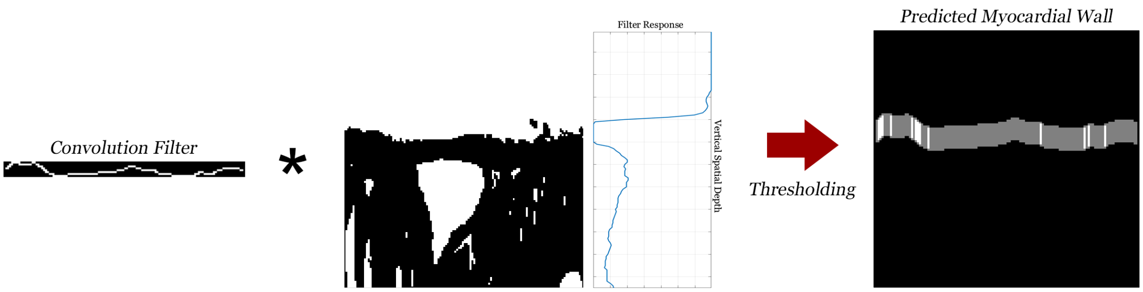

Figure 4: Convolution operation, followed by thresholding the low response, to extract the predicted myocardial wall in the ED mid-ventricular phase.

3 Results

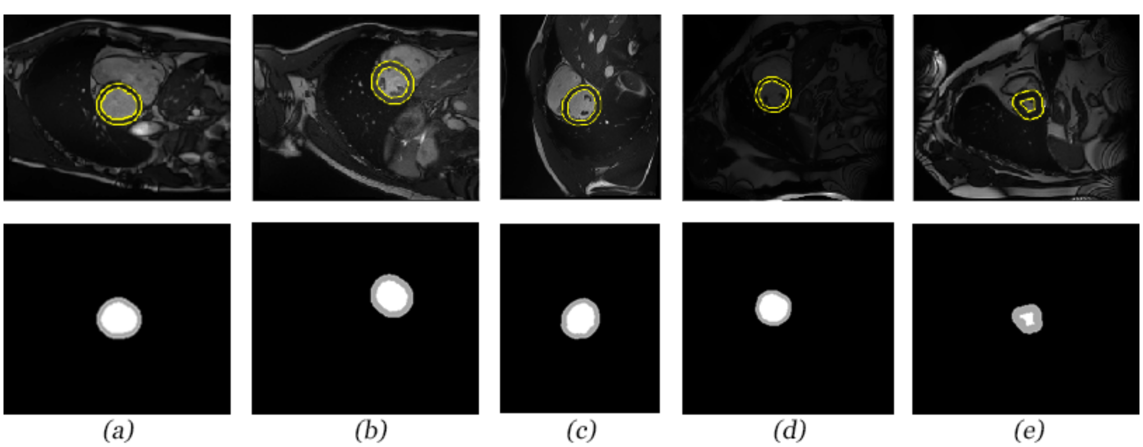

Figure 5: Segmented masks of the left ventricle and myocardium in ED mid-ventricular phase independently (below) and while overlaid on the target slice (above), for 5 distinct patient cases.

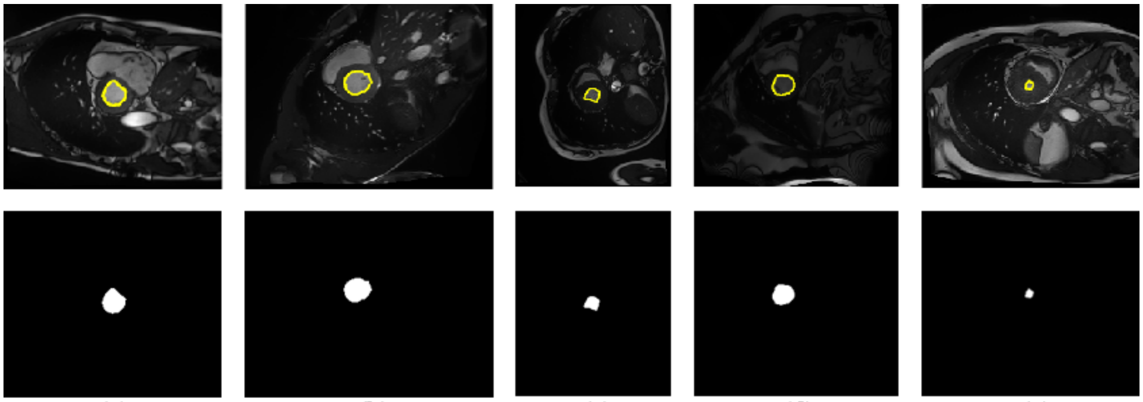

Figure 6: Segmented masks of the left ventricle in the ES mid-ventricular phase independently (below) and while overlaid on the target slice (above), for 5 distinct patient cases.

Table 1: Evaluation metrics for the ACDC 2017 training dataset, where Min', Max', $Mean'$ refer to evaluation of all definitive results (96 out of 100 cases)

		Dice Index			
Structure	Mid-Phase	Max	Min'	$Mean$	$Mean'$
Left Ventricle	ED	0.9870	0.7194	0.9040	0.9334
	ES	0.9751	0.2771	0.8134	0.8473
Myocardium	ED	0.9808	0.3543	0.8784	0.9066

		Hausdorff Distance			
Structure	Mid-Phase	Max'	Min	$Mean$	$Mean'$
Left Ventricle	ED	12.0000	1.0000	5.7565	3.5667
	ES	18.7883	1.0000	6.7115	4.6508
Myocardium	ED	26.6833	1.4142	6.5172	4.1834

4 Conclusion

4.1 Discussion

In Fig 5 & 6, we can see examples of the segmented mid-ventricular masks generated in ED and ES using our method. Although, the roundness metric is an important parameter for selecting the correct object during segmentation, the proposed method is proficient in generating a **suitable mask for an irregular LV** in both ED [Fig 5:*(e)*] and ES [Fig 6:*(c)*] as well. This is because our evaluation of the roundness metric is actually weighted to select an object with the compact factor of an LV, while still considering its relative area in comparison to surrounding side-components. Additionally, the method can also **detect and segment the target object in a dark image** [Fig 5:*(d)*, Fig 6:*(d)*] **and a very small LV**

cavity [Fig 6:*(e)*]. Table 1 highlights these results through the Dice Index and Hausdorff Distance (calculated via MATLAB [7] [8]).

4.2 Limitations

The proposed method is susceptible to drawbacks. It is still unable to segment the myocardium in ES with significant accuracy, as a result of which, this functionality has been skipped in the current version. Finally, its accuracy pales in comparison to the flexibility and computational power of modern deep learning algorithms used in practical applications [9]. In fact, the evaluation metrics themselves are still defined for a training set, and hence, can only be a reliable measure pending evaluation on a testing set. That being said, the current version of the program also incorporates a graphical user interface as a significant complement for any user to test the algorithm on the 2017 MICCAI ACDC training set.

5 References

[1] *Automated Cardiac Diagnosis Challenge - ACDC* (2019) [ONLINE] Available: `https://acdc.creatis.insa-lyon.fr/` [Accessed 05 January 2019]

[2] Ilias, Grinias, Tziritas, Georgios (2018) *"Fast Fully-Automatic Cardiac Segmentation in MRI Using MRF Model Optimization, Substructures Tracking and B-Spline Smoothing"*, MICCAI. DOI: 10.1007/978-3-319-75541-0_10

[3] Chan T. F., Vese L. A. (2001) *"Active contours without edges"*, IEEE Transactions on Image Processing 10, 266-277

[4] Petitjean, C., Dacher, J. (2011) *"A review of segmentation methods in short axis cardiac MR images"*, Medical Image Analysis, Elsevier. DOI: 10.1016/j.media.2010.12.004

[5] Tartar, A., Kilic, N., Akan, A. (2013) *"Classification of Pulmonary Nodules by Using Hybrid Features"*, Computational and Mathematical Methods in Medicine. DOI: 10.1155/2013/148363

[6] Canny, J. (1986) *"A Computational Approach To Edge Detection"*, IEEE Trans. Pattern Analysis and Machine Intelligence, 8(6):679–698

[7] *Sørensen-Dice Similarity Coefficient for Image Segmentation - MATLAB MathWorks France* (2017) [ONLINE] Available: `https://fr.mathworks.com/help/images/ref/dice.html` [Accessed 05 January 2019]

[8] *Hausdorff Distance - File Exchange - MATLAB* (2011) [ONLINE] Available: `https://fr.mathworks.com/matlabcentral/fileexchange/26738-hausdorff-distance` [Accessed 05 January 2019]

[9] Bernard O.,Lalande A., Zotti C., et al.(2018) *"Deep Learning Techniques for Automatic MRI Cardiac Multi-structures Segmentation and Diagnosis: Is the Problem Solved?"* IEEE Transactions on Medical Imaging. DOI: 10.1109/TMI.2018.2837502